

# Thermostimulative Shape Memory Effect of Linear Low-Density Polyethylene/Polypropylene (LLDPE/PP) Blends Compatibilized by Crosslinked LLDPE/PP Blend (LLDPE-PP)

Hong Liu, Shu-Cai Li, Yi Liu, Mahmood Iqbal

School of Material Science and Chemical Engineering, Tianjin University of Science and Technology, Tianjin 300457, China

Received 8 December 2010; accepted 20 February 2011

DOI 10.1002/app.34345

Published online 22 June 2011 in Wiley Online Library (wileyonlinelibrary.com).

**ABSTRACT:** A novel linear low-density polyethylene (LLDPE)/polypropylene (PP) thermostimulative shape memory blends were prepared by melt blending with moderate crosslinked LLDPE/PP blend (LLDPE-PP) as compatibilizer. In this shape memory polymer (SMP) blends, dispersed PP acted as fixed phase whereas continuous LLDPE phase acted as reversible or switch phase. LLDPE-PP improved the compatibility of LLDPE/PP blends as shown in scanning electron microscopic photos. Dynamic mechanical analysis test showed that the melt strengths of the blends were enhanced

with increasing LLDPE-PP content. A shape memory mechanism for this type of SMP system was then concluded. It was found that when the blend ratio of LLDPE/PP/LLDPE-PP was 87/13/6, the blend exhibited the best shape memory effect at stretch ratio of 80%, stretch rate of 25 mm/min, and recovery temperature of 135°C. © 2011 Wiley Periodicals, Inc. *J Appl Polym Sci* 122: 2512–2519, 2011

**Key words:** shape memory; blends; linear low-density polyethylene; polypropylene; compatibilization

## INTRODUCTION

Thermostimulative shape memory polymers (TSMPS) are those that have the capability of changing their shapes from a temporary shape to a permanent shape on application of an external thermal stimulus.<sup>1</sup> It attracts great attention of scientists and engineers due to the novel capacity, which can be designed into one temporary shape and then recovered to original shape when temperature varies from below to above the transition temperature. Over shape memory metallic alloys and shape memory ceramics, TSMPS have the advantages of light weight, low cost, good processability, high shape deformability, high shape recoverability, and tailorable switch temperature.<sup>2–4</sup> Therefore, it provides greatly potential values for applications in sensors, microelectromechanical systems, packaging, biomedical devices, fabrics, etc.<sup>5–10</sup>

TSMPS generally consist of two phases,<sup>11,12</sup> one is a fixed phase for memorizing original shape and the other one is a reversible phase for changing and recovering its shape. Generally, the fixed phase can be chemical or physical crosslinking structures,

whereas the reversible phase can be either crystalline or amorphous structure.

To our knowledge, the preparations of TSMPS can be classified into two main categories. One is chemical synthesizing copolymer that includes hard and soft segments, for example, polyurethanes,<sup>13–15</sup> and the other is polymer blending. Compared to the chemical synthesis, polymer blending offers a much simpler way to fabricate TSMPS. Recently, studies on the thermostimulate shape memory blends have been received much more academic interests.<sup>16–18</sup> Zhang et al.<sup>19</sup> found that melt blending of polylactide (PLA) and polyamide elastomer (PAE) had been performed in an effect to toughen the PLA; meanwhile, the PAE/PLA blends exhibited good shape memory effect. Chang et al.<sup>20</sup> studied a novel SMP which was prepared by blending of end-carboxylated telechelic poly( $\epsilon$ -caprolactone) (XPCL) and epoxidized natural rubber (ENR). The XPCL/ENR blends can form crosslinked structure via interchain reaction between the reactive groups of each polymer during melt blending; thus, the blends possessed excellent shape memory properties.

Polyolefin [e.g., polyethylene, polypropylene (PP)] that possess excellent mechanical properties belong to general plastics. If a SMP was prepared with polyolefin, huge economical benefits must be gained due to the low cost and high application values. In our laboratory, polyethylene has been taken as matrix

Correspondence to: Shu-Cai Li (lishuc@tust.edu.cn).

to prepare thermostimulate shape memory blends. Li et al.<sup>21</sup> prepared high-density polyethylene (HDPE)/poly(ethylene terephthalate) (PET) blends with ethylene-butyl acrylate-glycidyl methacrylate terpolymer as a reactive compatibilizer. The PET is used as the fixing phase and the HDPE matrix as the reversible phase. HDPE/PET blends exhibits good shape memory effects. The compatibilizer not only increases the compatibility but also increases the shape memory properties of the blends.

It is well known that the melting point of PP (165°C) is about 40°C higher than that of linear low-density polyethylene (LLDPE, 122°C). According to the shape memory mechanism of TSMP, LLDPE should act as the reversible phase, whereas the dispersed PP domains act as the fixed phase. Thus, a new SMP composed of LLDPE and PP can be prepared, if the interfacial adhesion of their blends is improved by adding proper amounts of compatibilizer. To our knowledge, it is never seen in past report to study the shape memory properties of LLDPE/PP blends. Our previous studies<sup>22</sup> had shown that moderate crosslinked LLDPE/PP blends (LLDPE-PP) could enhance the interfacial adhesion between LLDPE and PP and improve the mechanical properties of LLDPE/PP blends. In this article, we prepared LLDPE/PP blends by melt extrusion with LLDPE-PP as compatibilizer, and the effects of blend ratios, deformation conditions, and recovery temperatures on the shape memory behavior of LLDPE/PP/LLDPE-PP blends were investigated. Finally, a shape memory mechanism for this type of SMP blend was proposed.

## EXPERIMENTAL

### Materials

LLDPE (DGM-1820) with a density of 0.92 g/cm<sup>3</sup> and a melt flow rate (MFR) of 0.51 g/10 min (ASTM D1238, 190°C, 2.16 kg) produced by Petro-Chemical Corp. (Tianjin, China). PP (T30s) with a density of 0.9 g/cm<sup>3</sup> and a MFR of 3.6 g/10 min (230°C, 2.16 kg) were produced by Petro-Chemical Corp. Benzoyl peroxide (BPO, the initiator) was of analytical grade and produced by Tianlian Fine Chemical Corp.

### Preparations

Preparation of LLDPE-PP used as compatibilizers

The crosslinking of LLDPE/PP blend (LLDPE/PP ratio: 70/30) was carried out in a Haake mixer (PolylabRC.300P, Thermal Electron, Germany) using 0.4 wt % of BPO in the blends. Before the reactive melt blending, BPO was dissolved in acetone and then mixed with LLDPE and PP granules. After volatilizing the acetone, BPO adhered onto the granules

homogeneously. The temperature of mixing chamber was 180°C, the rotation speed was 60 rpm, and the selected mixing time was 3.5 min. After cooling, the LLDPE-PP melt was broken into granules and dried (12 h, 60°C) in a vacuum oven. The MFR of LLDPE-PP was 0.2 g/10 min (230°C, 2.16 kg). According to ASTM D2765, the gel content of LLDPE-PP was 3.75%.

### Preparation of LLDPE/PP/LLDPE-PP ternary blends

LLDPE/PP blends with and without the LLDPE-PP were prepared by melt extrusion, which was carried out in a single-screw extruder (PLE330 Brabender OHG, Duisburg, Germany) with a diameter of 19 mm and a length-to-diameter ratio (L/D) of 25. LLDPE, PP, and LLDPE-PP in a given ratio were introduced into the hopper of the extruder at a screw speed of 35 rpm and barrel temperatures (from the feeding zone to the die) of 160, 180, 200, and 190°C. The extrudate was cooled in air, cut into pellets, and dried for 12 h at 60°C.

The standard dumbbell specimens for the measurements of shape memory properties were made through an injection molding machine (JPH50, ONLY, Guangdong, China) with screw diameter of 28 mm, length-to-diameter ratio (L/D) of 21, temperatures (from hopper to nozzle) of 180, 195, 210, and 200°C, temperature of 25°C at mold, and injection pressure of 45 MPa. The period of time for cooling was 25 s.

### Characterizations and measurements

Injection-molded sample was used to investigate the phase structures of these blends. The specimens were cryogenically fractured in liquid nitrogen and sputter coated with Au. All of the SEM images were observed on a scanning electron microscopy (SEM; JSM-6380, JEOL, Japan).

Dynamical mechanical tests were performed by using a dynamic mechanical analyzer (DMA2980, TA Instruments; Newcastle, DE) in a tensile mode at the frequency of 1 Hz. The temperature was increased at the heating rate of 3 °C/min in the range of 60–60°C.

Shape memory test was carried out according to the follow steps. (1) Two distance lines of approximately 20 mm were drawn at the center of a dumbbell specimen, and the distance between the two lines was measured accurately and recorded as  $L_0$ . (2) The specimen was clamped in the heating chamber of universal testing machine (CMT4503 SANS Testing Machine; Shenzhen, China), heated up to the deformation temperature (130°C), and was holded for 5 min. (3) The specimen was stretched at a given stretch rate (e.g., 25 mm/min) to the required length

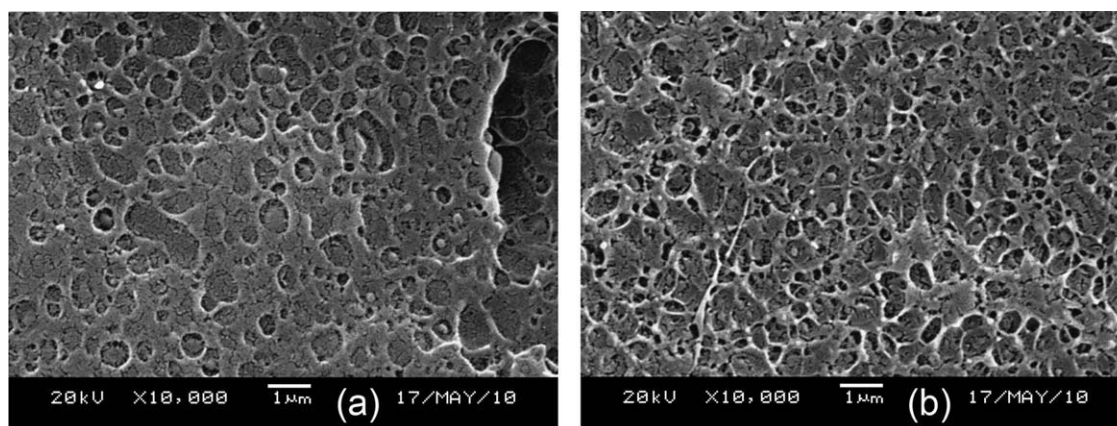


**Figure 1** SEM photographs of fracture surfaces of the blends: (a) LLDPE/PP (87/13) and (b) LLDPE/PP/LLDPE-PP (87/13/6).

with a given stretch ratio (e.g., 80%), then it was cooled to 23°C immediately to keep the deformation. The distance between the two lines in the stretch state was measured and recorded as  $L_1$ . (4) The stretched specimen was kept in 23°C for 24h, and recorded the distance  $L_2$ . (5) The stretched specimen was put into the oil bath at the response temperature without constraint. The recovery time ( $t$ ) was recorded when the deformed sample maximally reverted to the original shape, then the specimen was taken out and measured the distance recorded as  $L_3$ . Shape fixity ratio ( $R_f$ ) and shape recovery ratio ( $R_r$ ) were calculated by the following equations. Five samples were measured to achieve the average  $R_f$  and  $R_r$ .

$$R_f(\%) = \frac{L_2 - L_0}{L_1 - L_0} \times 100 \quad (1)$$

$$R_r(\%) = \frac{L_2 - L_3}{L_2 - L_0} \times 100 \quad (2)$$

## RESULTS AND DISCUSSION

### Phase structure

SEM micrographs of the cryogenic fracture surfaces of the various LLDPE/PP/LLDPE-PP blends are shown in Figure 1. As shown, the blends had two phases obviously. The droplets of PP dispersed in the continuous matrix of LLDPE. For LLDPE/PP binary blend [Fig. 1(a)], the phase morphology displayed just a little interface adhesion between LLDPE and PP. The size of dispersed particles was not uniform, and some of them became large. The similar structure was reported elsewhere.<sup>23</sup> When adding 6 phr of LLDPE-PP [Fig. 1(b)], PP particle size was decreased significantly and the interface adhesion between these two phases was enhanced. It indicated that LLDPE-PP as compatibilizer improved the com-

patibility of LLDPE/PP blends due to the same structures of two sides of LLDPE-PP to that of LLDPE and PP, respectively.

### Dynamic mechanical analysis

Figure 2 presents the temperature dependence of storage modulus ( $E'$ ) for pure LLDPE, LLDPE/PP, and LLDPE/PP/LLDPE-PP, respectively. As shown, in Figure, the modulus of all samples decreased slowly along with temperature below 120°C, and then descended abruptly when the temperature reached to 122°C, which was attributed to the melting of the crystalline LLDPE. It was worth of notice that pure LLDPE had lost its strength wholly when the temperature was above 125°C, but the blends still kept certain strength until the temperature increased to 160°C. Moreover, the high elastic modulus in the plateau region of the LLDPE/PP/LLDPE-PP blends increased with increasing LLDPE-PP content. All

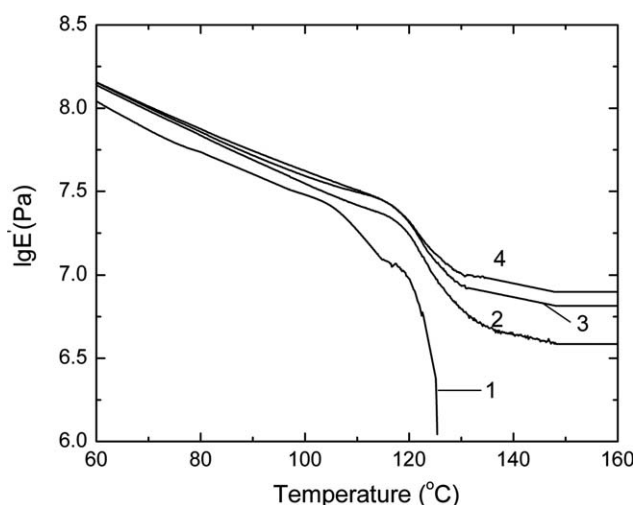


**Figure 2** Relationship between storage modulus ( $E'$ ) and the temperature of LLDPE/PP/LLDPE-PP blends: (1) pure LLDPE; (2) 87/13/0; (3) 87/13/2; and (4) 87/13/6.

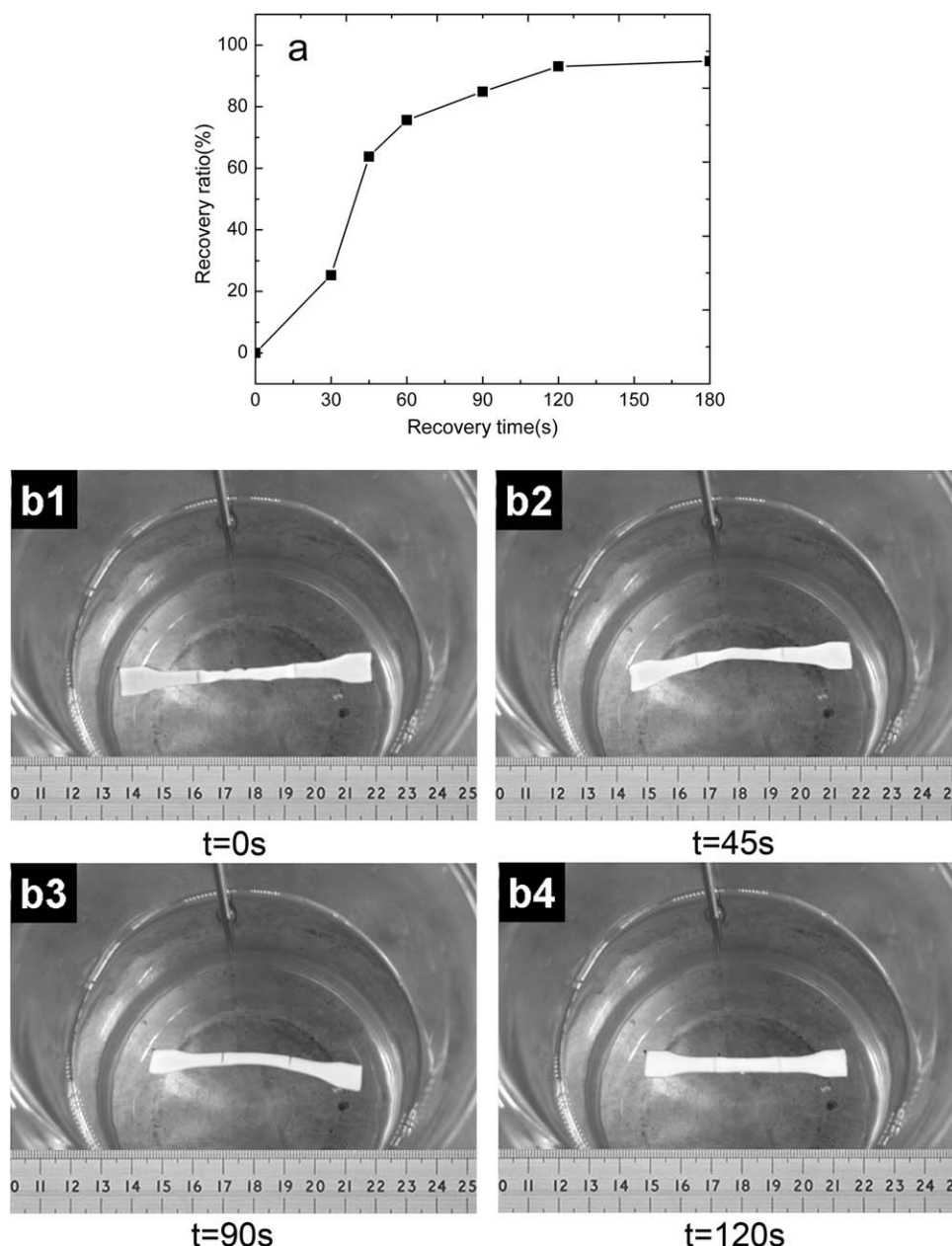


**Figure 3** Thermostimulative shape-memory recovery process of LLDPE/PP/LLDPE-PP (87/13/6) blends at 135°C: (a) shape recovery ratio-time curve; (b) recovery process;  $t$ , the recovery time.

these results indicated that in LLDPE/PP blends, the PP domains dispersed uniformly in the LLDPE matrix may act as physical crosslink points. With the addition of compatibilizer, the interaction between these two phases was enhanced and more stable physical network structures were formed.

#### Shape recovery process

Figure 3 shows thermostimulative shape memory recovery process of LLDPE/PP/LLDPE-PP (87/13/6) blend at 135°C. As shown in Figure 3(b1–b4), it took 120 s for the specimen recovered from the temporary shape (b1) to its initial shape (b4). The relationship

between recovery time and recovery ratio is shown in Figure 3(a). It was found that recovery ratio of the blend increased by increasing the recovery time and leveled off, when the time was above 120 s. In the beginning of recovery process (0–30 s), heat transferred from outside to inside the chains of the blends needed to take several seconds, so the recovery ratio increased slightly; in the 30–45 s range, the internal stress which frozen in system was rapidly released due to the increase of molecular chain movement, and the recovery ratio was raised sharply. After 120 s, shape recovery ratio leveled off as the internal stress kept in the blends was completely released.

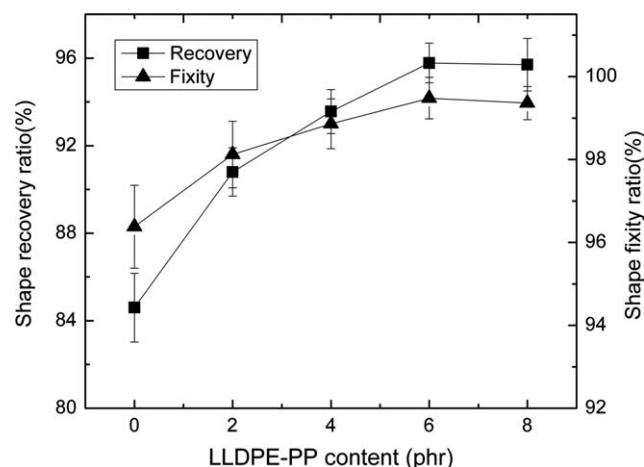


**Figure 4** Shape fixity ratio ( $R_f$ ) and shape recovery ratio ( $R_r$ ) of LLDPE/PP (87/13) blends as a function of LLDPE-PP concentration.

### Shape memory effects

#### Effect of the compatibilizer content

As shown in Figure 4, the  $R_f$  and  $R_r$  values of LLDPE/PP binary blends were low. With increasing LLDPE-PP content, the  $R_f$  and  $R_r$  values of LLDPE/PP/LLDPE-PP blends obviously increased and reached the maximum when the concentration of LLDPE-PP was 6 phr. The  $R_f$  and  $R_r$  values of LLDPE/PP binary blends were low due to the insufficient interface adhesion between LLDPE and PP phases. With the addition of LLDPE-PP, the interaction between LLDPE and PP phases was enhanced, so that PP dispersed in the LLDPE matrix acted effectively as fixed phase. Moreover, the high elastic modulus of the LLDPE/PP/LLDPE-PP blends increased with increasing LLDPE-PP LLDPE-PP content (Fig. 2). Under the same deformation conditions for the shape memory test, the internal stress frozen in system was greater due to the larger high elastic modulus of the blends; thus, the shape recovery force was enhanced during the recovery process. This led to the improvement of shape memory effect for LLDPE/PP/LLDPE-PP blends.

#### Effect of the PP content

When the content of LLDPE-PP was fixed at 6 phr, the effects of the PP content on the  $R_f$  and  $R_r$  values of LLDPE/PP/LLDPE-PP blends are shown in Figure 5. It was found that the  $R_f$  value of LLDPE/PP/LLDPE-PP blends increased with increasing PP content. When the concentration of PP exceeded 13 phr, the  $R_f$  value leveled off and was close to 100%. It could be attributed to the fact that when PP content was too low (5 phr), the constraint force which PP phase acted on reversible phase was insufficient. With increasing PP content, the PP as fixed phase

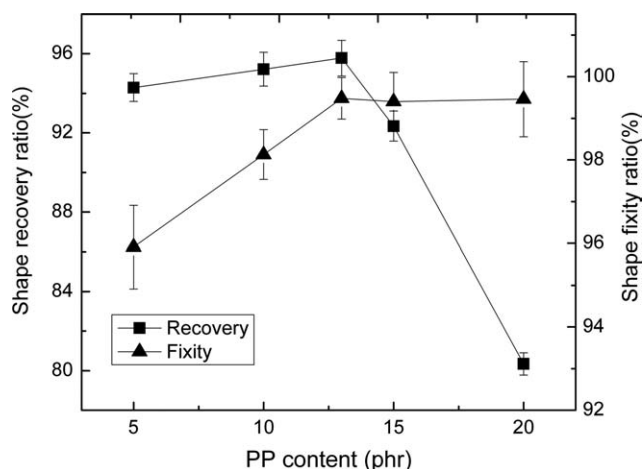


**Figure 5** Shape fixity ratio ( $R_f$ ) and shape recovery ratio ( $R_r$ ) of LLDPE/PP/LLDPE-PP blends as a function of PP concentration.

acted to LLDPE was enhanced due to the increase of physical crosslink points in LLDPE/PP blends; thus, the  $R_f$  value of the blends was enhanced. However, when PP content exceeded 13 phr the  $R_r$  value of the blends rapidly decreased. Because of the relatively less content of the reversible phase, the irreversible plastic deformation was prone to occur under the same deformation conditions, which led to the reduction of shape recovery ratio of the blends.

#### Effect of recovery temperature

Figure 6 displayed the variation of  $R_r$  values with temperature for the LLDPE/PP/LLDPE-PP LLDPE-PP (87/13/6) blends. As shown, the  $R_r$  values were low when the temperature was below 120°C and

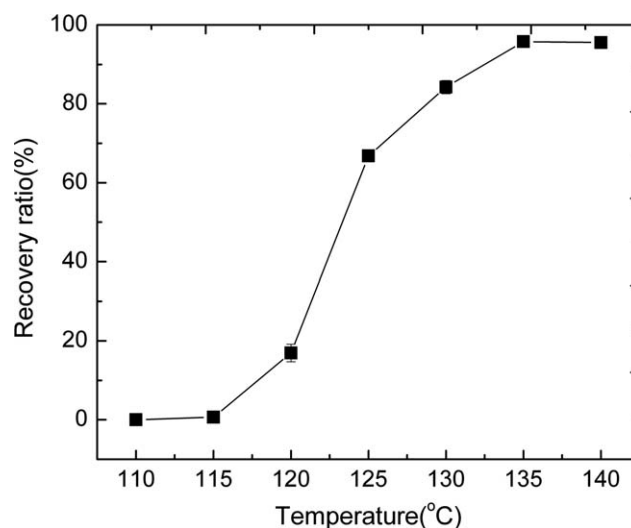


**Figure 6** Variation of shape recovery ratio with temperature for the LLDPE/PP/LLDPE-PP (87/13/6) blends.

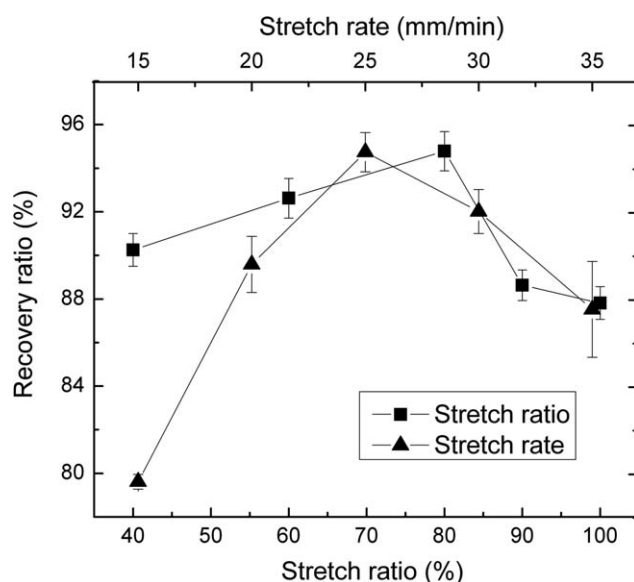


**Figure 7** Relationship between shape recovery ratio and deformation conditions such as stretch ratios and stretch rates for LLDPE/PP/LLDPE-PP (87/13/6) blends under response temperature (135°C).

then ascended sharply at about 120–130°C. The  $R_r$  values were high and leveled off when the temperature was above 135°C. It was worth noting that the  $R_r$  values of LLDPE/PP blends increased obviously when the temperature was close to the melting point of LLDPE. As a result, the best shape response temperature of LLDPE/PP/LLDPE-PP blends was dependent on the melting point of the reversible phase and a little more than that of temperature. The similar result was reported by Li et al.<sup>21</sup>

#### Effect of deformation conditions

Deformation conditions which included stretch ratios and stretch rates had great influence in the shape recovery ratio ( $R_r$ ) of the blends. As shown in Figure 7, under the same conditions, the  $R_r$  value of the blends increased initially and then decreased with increasing stretch ratio. The shape recovery ratio was highest at the stretch ratio of 80%. This could be explained that when the stretch ratio below 80%, the degree of orientation of LLDPE molecular chains increased with increasing the stretch ratio, so that the recoverable deformation and the recovery stress which kept in the system were increased. However, when the stretch ratio exceeded 80%, irreversible slip between LLDPE molecular chains might begin with further increase of deform ratio and then the shape recovery ratio would be reduced. An interesting observation from Figure 7 was that the effects of stretch rate on  $R_r$  value of the blends had the similar trend to that of stretch ratio. When the stretch rate was 25 mm/min, the  $R_r$  value of the blends reached the maximum. The shape memory

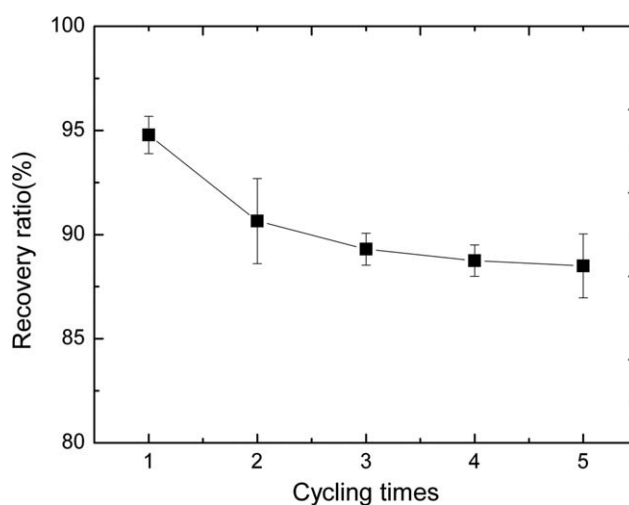


**Figure 8** Effects of cycling times on recovery ratio of LLDPE/PP/LLDPE-PP (87/13/6) blends.

effect of polymers depend on the internal stress when frozen in the system, but the stress relaxation of polymer molecular chains would reduce the internal stress before the specimens were frozen. Thus, shortening time for external stress acted to specimens could enhance the shape memory effect due to the reduction of the stress relaxation.<sup>24</sup> Therefore, when the stretch rate was below 25 mm/min, the  $R_r$  values of the blends increased with increasing stretch rates. But when the stretch rate was overlarge, the molecular chains of the blends might be destroyed. Thus, the shape recovery ratio of the blends was reduced.

The shape recovery ratios decreased slightly as the cycling times increased, as shown in Figure 8. This is due to the accumulation of plastic deformations. The plastic deformations which inevitably occurred

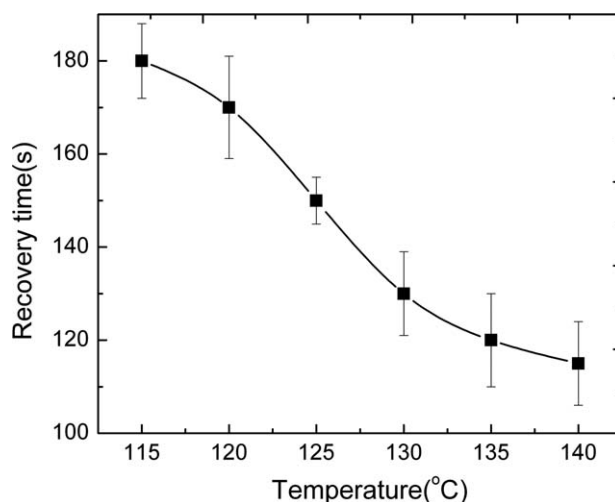


**Figure 9** Relationship between shape recovery ratio and recovery temperature for LLDPE/PP/LLDPE-PP (87/13/6) blends.

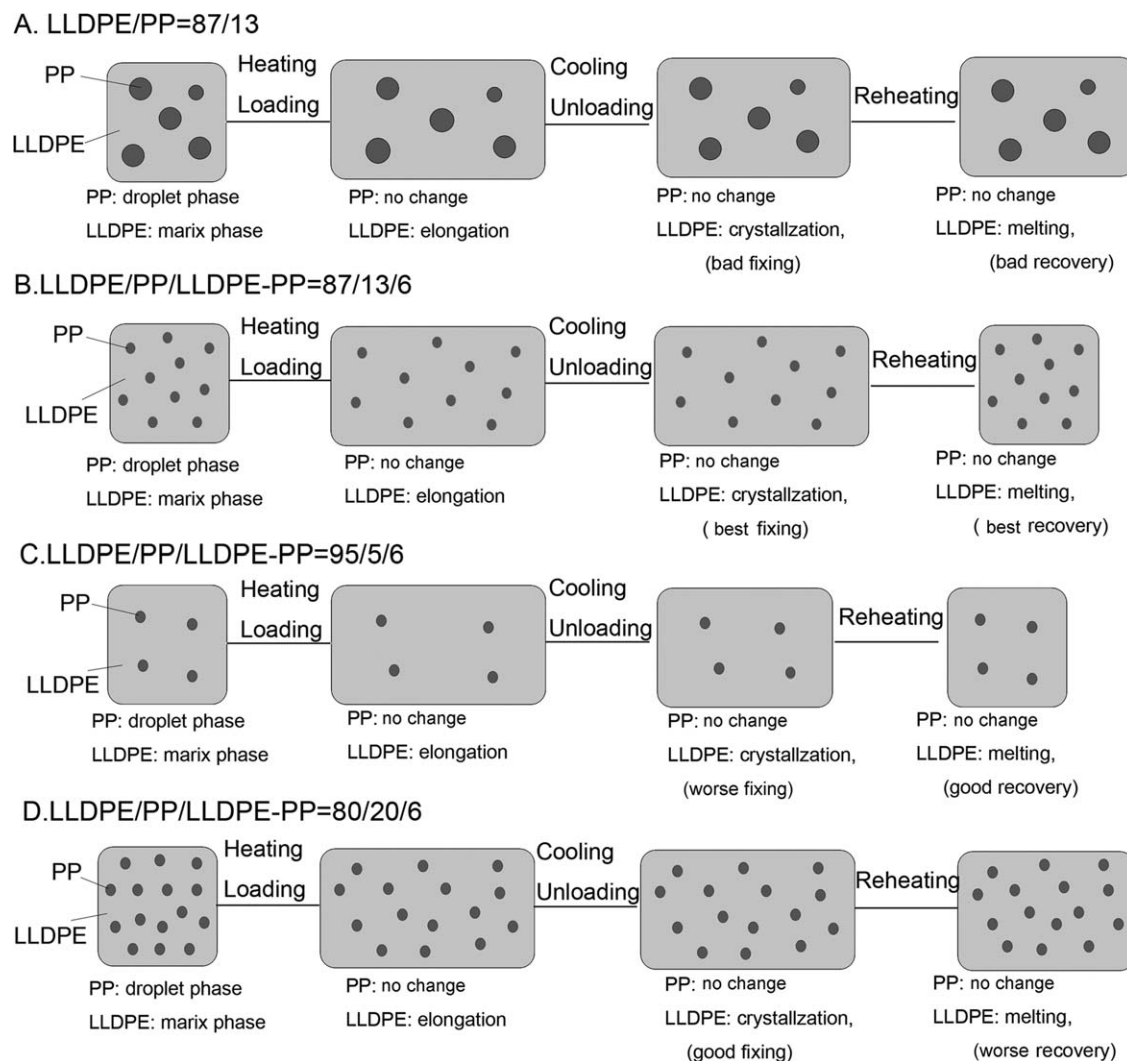


**Figure 10** Schematic figures of the shape memory mechanism of LLDPE/PP/LLDPE-PP blends.

during each recovery test led to the reduction of shape memory effect of the blends.

### Shape recovery speed

The shape recovery speed was expressed by the time when SMP reached the maximum recovery ratio. Figure 9 presents the relationship between recovery temperature and shape recovery time for LLDPE/PP/LLDPE-PP (87/13/6) blends. It was found that shape recovery time of the blends decreased gradually with increasing the recovery temperature, indicating that shape recovery speed got accelerated. According to the time-temperature equivalence principle,<sup>25</sup> the molecular motion was faster as the recovery temperature was higher, so that the shape recovery time became shorter. It was meant that shape recovery speed was increased with increasing the recovery temperature.

### Mechanism of shape memory properties of LLDPE/PP/LLDPE-PP blends

In LLDPE/PP/LLDPE-PP blends, dispersed PP phase acted as fixed phase while the LLDPE matrix that have switch temperature acted as reversible phase. By heating the SMP to the switch transition temperature (130°C) of reversible LLDPE phase, PP crystalline region acted as the physical crosslink point to keep the original structure. On the other hand, deformation occurred to LLDPE phase involving molecular orientation during stretch process at the switch temperature. After unloaded and cooled, the elongation shape was kept and the internal stress was stored in the system. Thus, the molecules regained the activity and recovered to their original shape with the internal stress releasing instantaneously at the shape response temperature, as shown in Figure 3.

Figure 10 presented the schematic figures of the shape memory mechanism of LLDPE/PP/LLDPE-PP LLDPE-PP blends. For LLDPE/PP binary blend,

both bad shape fixity performance and bad shape recovery performance were shown in Fig. 10(a), which was due to the insufficient restraint force that PP fixed phase acted to reversible LLDPE phase. After adding the compatibilizer [Fig. 10(b)], the droplets of PP dispersed more uniformly in the continuous matrix of LLDPE, and the number of PP particles became larger and the size became smaller. The interaction between the fixed phase and reversible phase was enhanced so that the blends showed the best shape fixity and recovery performance. However, when PP content was too low [Fig. 10(C)], the blends exhibited good shape recovery performance but bad shape fixity performance, which was explained by the fact that the constraint effect that fixed phase acted on reversible phase was small due to the low concentration of fixed phase. On the contrary, when PP content was excessive [Fig. 10(D)], the blend showed good shape fixity performance, but because of the low content of reversible phase, the irreversible plastic deformation was prone to occur under the same deformation conditions, which led to the bad shape recovery effect. Consequently, when the blend ratio of LLDPE/PP/LLDPE-PP blends was 87/13/6, the blend possessed the best shape memory properties.

### CONCLUSIONS

LLDPE/PP/LLDPE-PP blends were prepared by melt blending with good shape memory properties. SEM photos showed that PP particles dispersed in LLDPE matrix and LLDPE-PP as compatibilizer not only improved the compatibility of LLDPE/PP blends but also enhanced the melt strengths of the blends as shown in DMA tests.

From the shape memory investigation results, a new shape memory mechanism for this type of ternary blend SMP was proposed, in which the two components that had quite different melting points contributed, respectively, to shape memory performance. One of them having higher melting point acted as a fixed phase and the other was the reversible or switch one, the third component acted as compatibil-

izer to improve the compatibility of the blends. For this type of thermostimulative shape memory blends, the strong interaction between the fixed and reversible phase and the appropriate blend ratios were the keys to the good shape memory effect of the blends. During the deformation process, the droplets of fixed phase were unchanged to keep the original shape, whereas the molecular orientation occurred in reversible phase and internal stress was kept in the system. Consequently, heating up the material and releasing the stress will deform the shape back to the original shape.

### References

1. Meng, Q. H.; Hu, J. L. *Compos Part A* 2009, 40, 1661.
2. Lendlein, A.; Kelch, S. *Angew Chem Int Ed Engl* 2002, 41, 2034.
3. Hornbogen, E. *Adv Eng Mater* 2006, 8, 101.
4. Monkman, G. J. *Mechatronics* 2000, 10, 489.
5. Ratna, D.; Karger-Kocsis, J. *J Mater Sci* 2008, 43, 254.
6. Lendlein, A.; Langer, R. *Science* 2002, 96, 1673.
7. Fortelny, I.; Michalkova, D.; Krulis, Z. *Polym Degrad Stabil* 2004, 85, 975.
8. Wache, H. M.; Tartakowska, D. J.; Hentrich, A. *J Mater Sci Mater Med* 2004, 14, 109.
9. Mondal, S.; Hu, J. L.; Zhu, Y. *J Membr Sci* 2006, 280, 427.
10. Gall, K.; Dunn, M. L.; Liu, Y. *Acta Mater* 2002, 50, 5115.
11. Liu, C.; Qin, H.; Mather, P. T. *J Mater Chem* 2007, 17, 1543.
12. Zhang, H.; Wang, H. T.; Zhong, W. *Polymer* 2009, 50, 1596.
13. Zhu, Y.; Hu, J. L.; Choi, K. F. *Polym Adv Technol* 2008, 19, 328.
14. Hu, J. L.; Yang, Z. H.; Yeung, L. *Polym Int* 2005, 54, 854.
15. Merline, J. D.; Reghunadhan, C. P.; Gouri, C. *J Appl Polym Sci* 2008, 107, 4082.
16. Wang, L. S.; Chen, H. C.; Xiong, Z. C. *Mater Lett* 2010, 64, 284.
17. Zhu, G. M.; Xu, S. G.; Wang, J. H. *Radiat Phys Chem* 2006, 75, 443.
18. Jeong, H. M.; Song, J. H.; Lee, S. Y. *J Mater Sci* 2001, 36, 5457.
19. Zhang, W.; Chen, L.; Zhang, Y. *Polymer* 2009, 50, 1311.
20. Chang, Y. W.; Eom, J. P.; Kim, J. G. *J Ind Eng Chem* 2010, 16, 256.
21. Li, S. C.; Lu, L. N.; Zeng, W. *J Appl Polym Sci* 2009, 112, 3341.
22. Li, S. C.; Liu, H.; Zeng, W. *J Appl Polym Sci*, to appear.
23. Jeong, H. G.; Lee, K. J. *Adv Polym Tech* 1999, 18, 43.
24. Rubinstein, M.; Colby, R. H. *Polymer Physics*; Oxford University Press: London, 2003.
25. Luo, W. B.; Yang, T. Q.; An, Q. L. *Acta Mech Solida Sin* 2001, 14, 195.